Electronic Supplementary Material (ESI) for Chemical Communications
This journal is © The Royal Society of Chemistry 2011

Cyclopenicillone, a Unique cyclopentenone from the Cultures of *Penicillium decumbens*

Electronic Supplementary Information

Sheng Lin,[‡,a] Ting Shi,[‡,b] Ke-Yv Chen,[a] Zhong-Xiao Zhang,[a] Yun-Heng Shen,[a] Lei Shan,[a] and Wei-Dong Zhang*[,a]

[a] *Department of Natural Product Chemistry, School of Pharmacy, Second Military Medical University, 325 Guohe Road, Shanghai 200433, China.*

[b] *Department of Pathophysiology, Key Laboratory of Cell Differentiation and Apoptosis of Chinese Ministry of Education, Shanghai JiaoTong University School of Medicine, Shanghai 200025, China.*

[‡] *These authors have contributed equally to this work.*

**** To whom correspondence should be addressed:*** *Fax: +86-21-81871244; Tel: +86-21-81871244; E-mail: wdzhangy@hotmail.com*

This journal is © The Royal Society of Chemistry 2011

Contents

Experimental Section

Computational Methods

Fig. S1. Key ^{1}H–^{1}H COSY (bold), HMBC (arrow) (left), and NOE correlations ( ) (right) for cyclopenicillone (**1**)

Fig. S2. Potential energy surface of cyclopenicillone (**1**) at the AM1 level in the gas phase.

Fig. S3. Optimized geometries of configurations of cyclopenicillone (**1**) at the B3LYP/6-31G** level in the gas phase.

Fig. S4. Optimized geometries of configurations of the C-1′ epimer (**2**) at the B3LYP/6-31G** level in the gas phase.

Fig. S5. Calculated ECD spectra of cyclopenicillone (**1**) at B3LYP/6-31G** level in gas phase and at B3LYP-SCRF/6-31G**//B3LYP/6-31G** level with the PCM model in methanol.

Fig. S6. Calculated ECD spectra of the C-1′ epimer (**2**) at B3LYP/6-31G** level in gas phase and at B3LYP-SCRF/6-31G**//B3LYP/6-31G** level with the PCM model in methanol.

Fig. S7. Calculated ECD spectra of cyclopenicillone (**1**) and the C-1′ epimer (**2**) in gas phase at B3LYP/6-311++G** level

Fig. S8. Calculated ECD spectra of cyclopenicillone (**1**) and the C-1′ epimer (**2**) at B3LYP-SCRF/6-311++G**//B3LYP/6-31G** level with the PCM model in methanol.

Fig. S9. Key molecular orbitals involved in the important transitions in ECD of conformer **2d** at B3LYP-SCRF/6-31G**//B3LYP/6-31G** level with the PCM model in methanol.

Table S1. Important dihedral angles of optimized cyclopenicillone (**1**) at B3LYP/6-31G** Level in the Gas Phase (Degree).

Table S2. Important thermodynamic parameters of cyclopenicillone (**1**) (au).

Table S3. Conformational analysis of cyclopenicillone (**1**).

Table S4. Important dihedral angles of optimized cyclopenicillone (**1**) and the C-1′ epimer (**2**) at B3LYP/6-31G** Level in the Gas Phase (Degree).

Table S5. Key transitions, oscillator strengths, and rotatory strengths in the ECD spectra of conformer **1a**, **1b**, **1c** and **1d** in the MeOH with PCM at B3LYP-SCRF/6-31G**//B3LYP/6-31G** Level.

Table S6. Key transitions, oscillator strengths, and rotatory strengths in the ECD spectra of conformer **2a**, **2b**, **2d** and **2f** in the MeOH with PCM at B3LYP-SCRF/6-31G**//B3LYP/6-31G** Level.

Table S7. The ihibitory activity of cyclopenicillone (**1**) against LPS-induced NO production in RAW264.7 macrophages.

Scheme 1. Postulated Biogenetic Formation of cyclopenicillone (**1**).

Fig. S10. The positive mode HRESI spectrum of cyclopenicillone (**1**).

Fig. S11. The IR spectrum of cyclopenicillone (**1**).

Fig. S12. The IR spectrum of cyclopenicillone (**1**) in a diluted concentration

Fig. S13. The ^{1}H NMR spectrum of cyclopenicillone (**1**) in MeOH-d_4.

Fig. S14. The ^{13}C NMR and DEPT spectra of cyclopenicillone (**1**) in MeOH-d_4.

Fig. S15. The ^{1}H-^{1}H COSY spectrum of cyclopenicillone (**1**) in MeOH-d_4.

Fig. S16. The HSQC spectrum of cyclopenicillone (**1**) in MeOH-d_4.

Fig. S17. The HMBC spectrum of cyclopenicillone (**1**) in MeOH-d_4.

Fig. S18. The ROESY spectrum of cyclopenicillone (**1**) in MeOH-d_4.

Experimental Section

General Experimental Procedures. Optical rotations were measured on a Perkin-Elmer 341 polarimeter. IR and UV spectra were recorded on Bruker Vector-22 and Shimadzu UV-2550 UV-visible spectrophotometers, respectively. NMR spectra were obtained on a Bruker Avance 600 MHz NMR spectrometer in MeOD. ESIMS and HRESIMS were acquired on an Agilent LC/MSD Trap XCT and a Q-TOF micro mass spectrometer (Waters, Milford, MA), respectively. Column chromatography (CC) was performed using Sephadex LH-20 (40-70 μm; Amersham Pharmacia Biotech AB, Uppsala, Sweden). Semipreparative HPLC was conducted on an ODS column (Kromasil, 5μm, 300×10 mm) using a PDA UV detector at 240 nm. TLC analysis was run on $HSGF_{254}$ silica gel plates (10-40 μm, Yantai, China).

Fermentation, Extraction, and Purification. The fungus strain LXY7-1 was isolated from the limestone soil collected from the limestone terrain Lingxiaoyan in Guangdong, China. It was identified according to its morphological characteristics and 18S RNA by Ke-Yv Chen, School of Pharmacy, Second Military Medical University, Shanghai, China. A voucher specimen is deposited in our laboratory at -80 ^{o}C. *Penicillium decumbens* LXY7-1 was cultured at 28 ^{o}C for 6 days while shaking at 165 rpm in 4 × 20 L volumes of the liquid medium (composed of 30 g of sucrose, 1 g of yeast extract, 3 g of $NaNO_3$, 0.5 g of $MgSO_4 \cdot 7H_2O$, 0.01 g of $FeSO_4 \cdot 7H_2O$, 1 g of K_2HPO_4, 0.5 g of KCl, per 1L of water, PH 6.5). The whole broth was filtered through cheesecloth to separate the broth supernatant and mycelia. The former was applied to an Amberlite XAD-16 macroporous adsorbent resin column. Elution of the column

with H_2O and MeOH (5 L each) yielded two corresponding residues after removing solvents. The MeOH residue (10.1 g) was suspended in H_2O (150 mL) and then partitioned with EtOAc (6 × 150 mL). The EtOAc extract was evaporated under reduced pressure to yield 2.5 g of residue, which was subjected to Sephadex LH–20 CC eluting with $CHCl_3$–MeOH (1:1) as eluent to produce four fractions (A-D). Fraction B was further fractionated by reversed-phase C-18 silica flash chromatography eluting with a step gradient from 20 to 80% MeOH in H_2O, to yield five subfractions (B1-B5). Subfractionn B2 was subjected to reversed-phase preparative HPLC (RP_{18}, 5 μm, 240 nm, MeCN–H_2O, 15:85) to afford **1** (1.5 mg).

Cyclopenicillone (**1**). Colorless soild; $[\alpha]_D^{20}$ +20.0 (*c* 0.08, MeOH); UV (MeOH) λ_{max} (log ε) 240 (3.90) nm; CD (MeOH) λ_{max} (Δε) 319.0 (–0.8), 240.0 (4.3), 210.0 (–1.2); IR (KBr) ν_{max} 3396, 2921, 1694, 1645, 1433, 1378, 1328, 1153, 1111, 1080, 1036 cm^{-1}; ^1H NMR and ^{13}C NMR data, see Table 1; ESIMS (positive) 225 $[M + H]^+$; ESIMS (negative) 223 $[M - H]^-$, 447 $[2M - H]^-$; HRESIMS (positive) $[M + H]^+$ *m/z* 225.1485, calcd for $C_{12}H_{21}O_3$, 225.1491.

This journal is © The Royal Society of Chemistry 2011

Biological Activity

Inhibitory activities against lipopolysaccharides (LPS)-induced nitric oxide (NO) production in RAW264.7 macrophages. RAW264.7 macrophages were seeded in 24-well plates (105 cells/well). The cells were co-incubated with drugs and LPS (1μg/mL) for 24h. The amount of NO was assessed by determined the nitrite concentration in the cultered RAW264.7 macrophage supernatants with Griess reagent. Aliqueots of supernatants (100 μL) were incubated, in sequence, with 50 μL 1% sulphanilamide and 50 μL 1% naphthylethylenediamine in 2.5% phosphoric acid solution. The absorbances at 570 nm were read using a microtiter plate reader.

MTT assay for cytotoxic activity in RAW264.7 macrophages. RAW264.7 macrophages were maintained in a water-saturated atmospheere of 5% CO_2 at 37 □. Experiments were carried out according to the reported protocol. The cell viability was evaluated by MTT [3-(4,5-dimethylthiazol-2-yl)-2,5-diphenyltetrazolium bromide, Sigma] reduction.

Reference:

(a) Denizot, F.; Lang, R. *J. Immunol. Methods* **1986**, *89*, 271−277.

(b) Qin, J. J.; Jin, H. Z.; Zhu, J. X; Fu, J. J.; Hu, X. J.; Liu, X. H.; Zhu, Y.; Yan, S. K.; Zhang, W. D. *Planta Med.* **2010**, *76*, 278−283

This journal is © The Royal Society of Chemistry 2011

Computational Methods

Original ECD data calculations

The energies, oscillator strengths and rotational strengths of the electronic excitations of all the conformers were calculated using the TDDFT methodology at the B3LYP/6-31G** level in the gas phase and at the B3LYP-SCRF/6-31G**//B3LYP/6-31G** level with the PCM model in methanol solution. The single point energies were also calculated at the B3LYP/6-311++G**//B3LYP/6-31G** level in the gas phase and at the B3LYP-SCRF/6-311++G**//B3LYP/6-31G** level with the PCM model in methanol solution. Rotational strengths are calculated using both length and velocity representations. All the calculations have been carried out with the Gaussian 09 program.

ECD simulation

The ECD spectra were then simulated by overlapping Gaussian functions for each transition according to:

$$\Delta\varepsilon(E) = \frac{1}{2.297\times10^{-39}} \times \frac{1}{\sqrt{2\pi\sigma}} \sum_{i}^{A} \Delta E_i R_i e^{-[(E-E_i)/(2\sigma)]^2}$$

Where σ is the width of the band at 1/e height and ΔE_i and R_i are the excitation energies and rotatory strengths for transition i, respectively, σ=0.20 eV and R^{len} have been used in this work.

To get the final spectra, all the simulated spectra of conformations of each compound were averaged according to their energy and the Boltzmann distribution theory expressed as:

$$\frac{N_i^*}{N} = \frac{g_i e^{-\varepsilon_i/k_B T}}{\sum g_i e^{-\varepsilon_i/k_B T}}$$

This journal is © The Royal Society of Chemistry 2011

Fig. S1. Key ^{1}H–^{1}H COSY (bold), HMBC (arrow) (left), and NOE correlations ( ) (right) for cyclopenicillone (**1**)

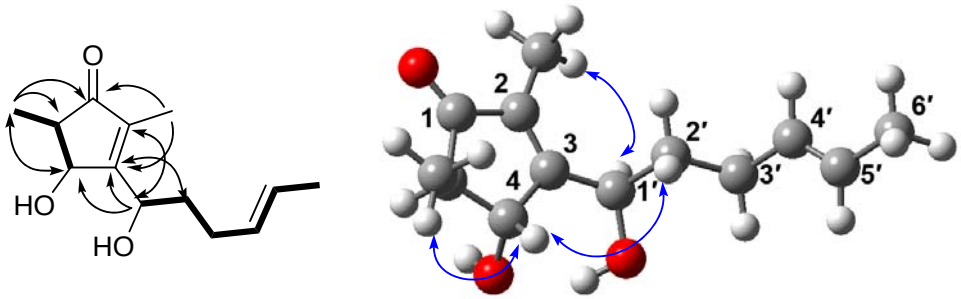

Fig. S2. Potential energy surface of cyclopenicillone (**1**) at the AM1 level in the gas phase.

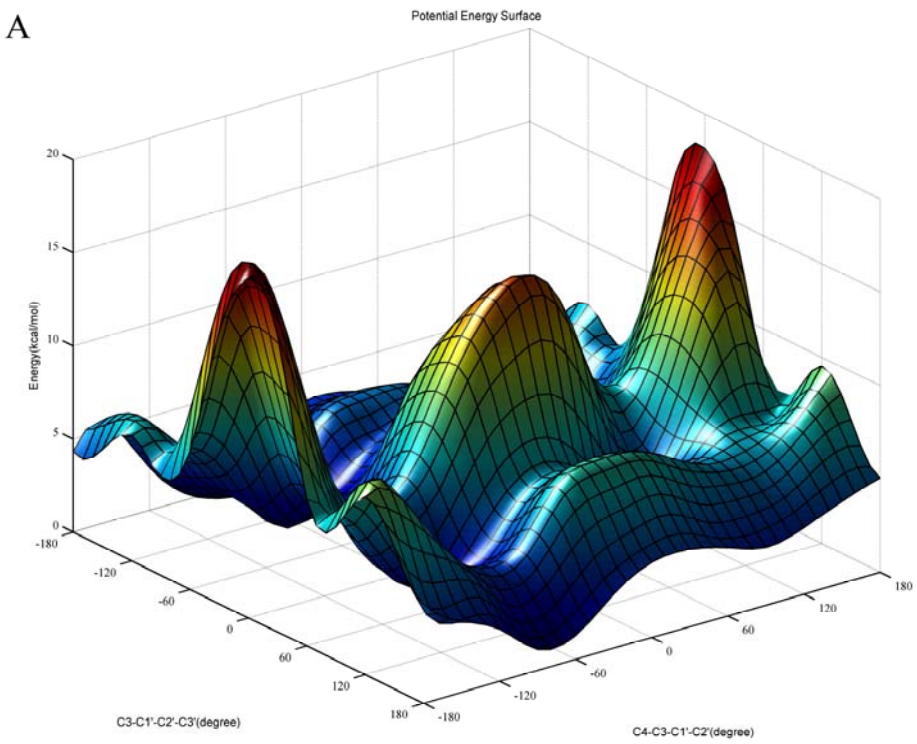

Fig. S3. Optimized geometries of configurations of cyclopenicillone (**1**) at the B3LYP/6-31G** level in the gas phase.

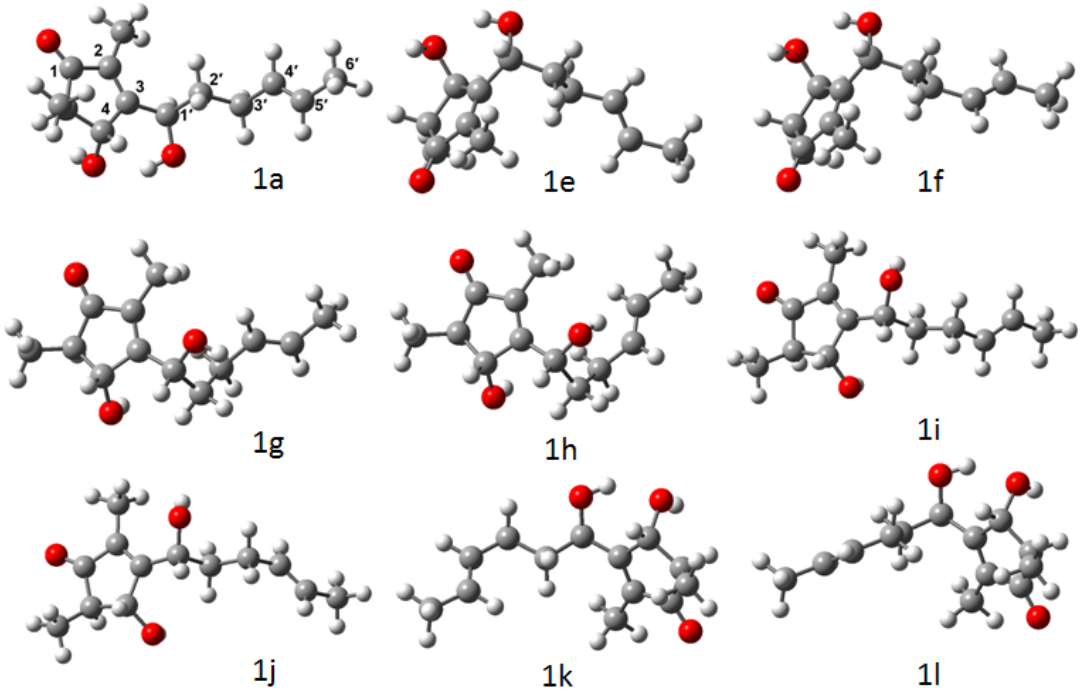

Fig. S4. Optimized geometries of configurations of the C-1′ epimer (**2**) at the B3LYP/6-31G** level in the gas phase.

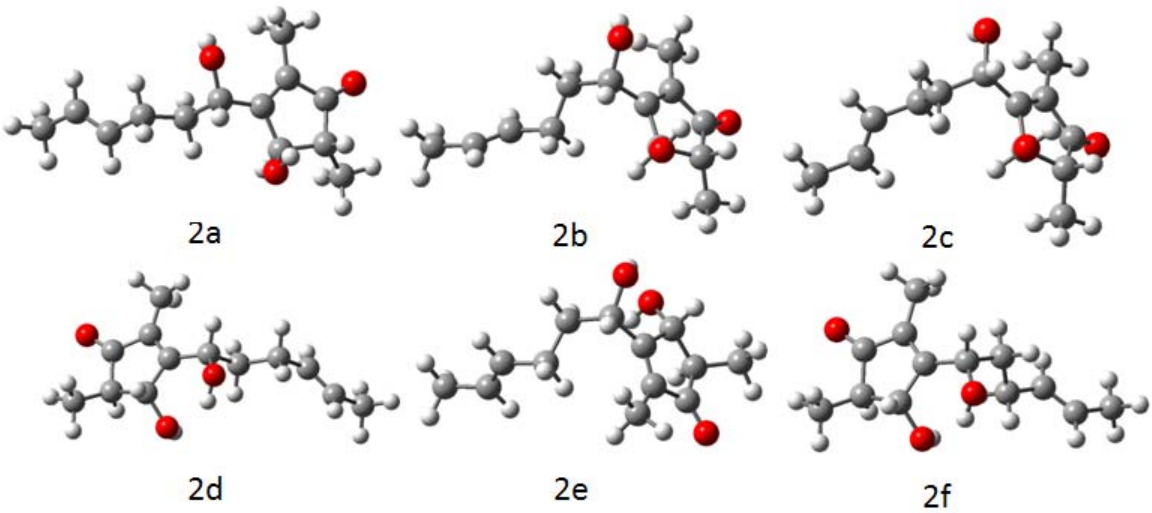

Fig. S5. Calculated ECD spectra of cyclopenicillone (**1**) at B3LYP/6-31G** level in gas phase and at B3LYP-SCRF/6-31G**//B3LYP/6-31G** level with the PCM model in methanol.

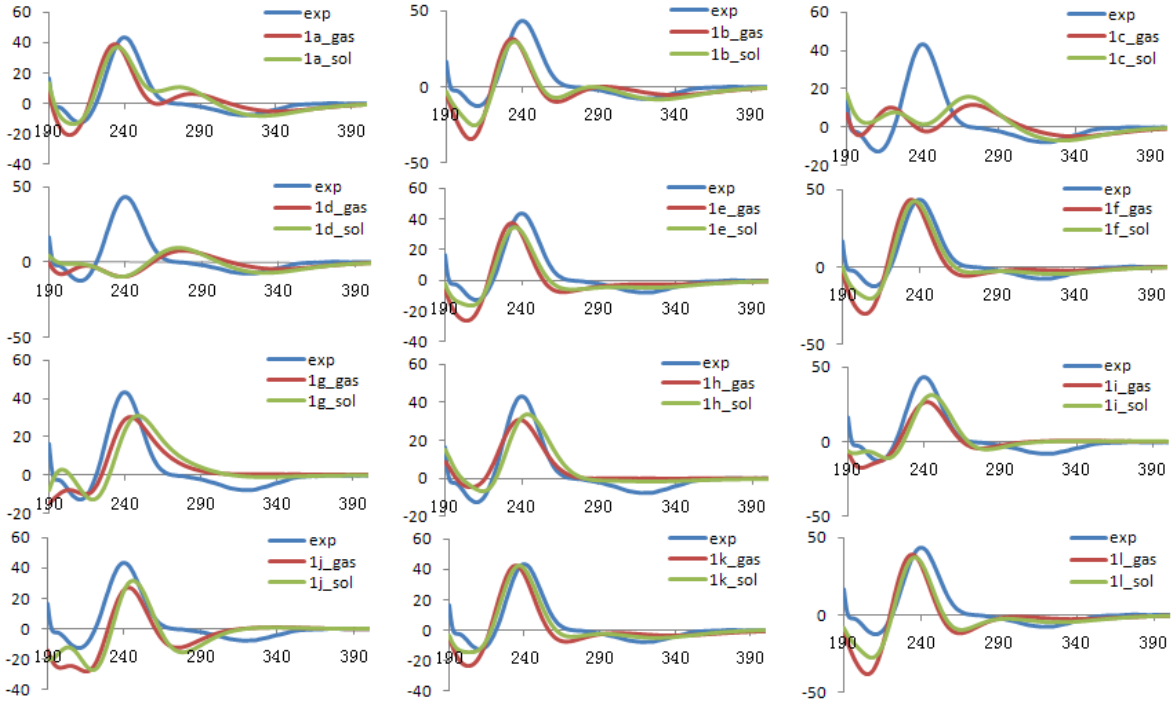

Fig. S6. Calculated ECD spectra of the C-1′ epimer (**2**) at B3LYP/6-31G** level in gas phase and at B3LYP-SCRF/6-31G**//B3LYP/6-31G** level with the PCM model in methanol.

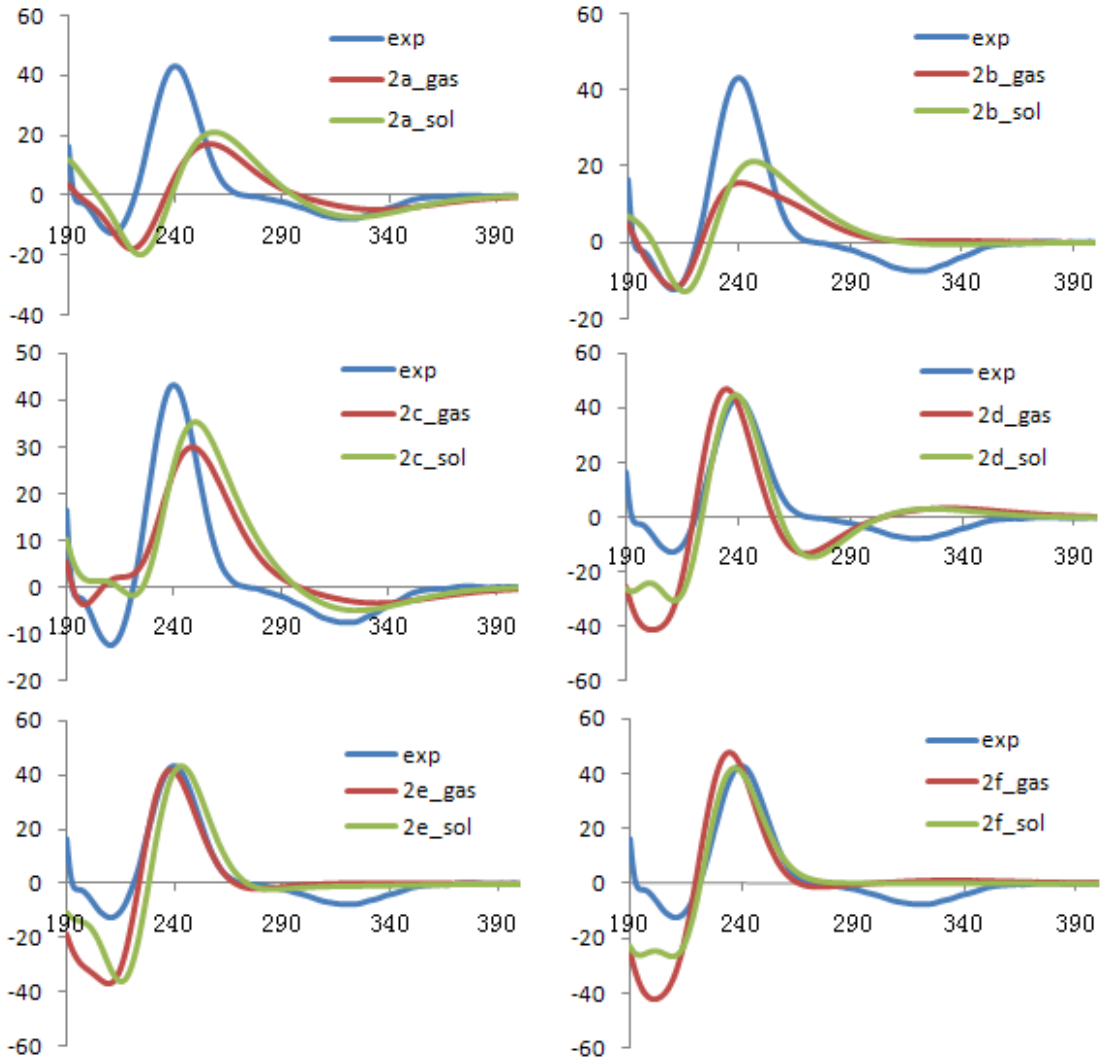

Fig. S7. Calculated ECD spectra of cyclopenicillone (**1**) and the C-1′ epimer (**2**) in gas phase at B3LYP/6-311++G** level

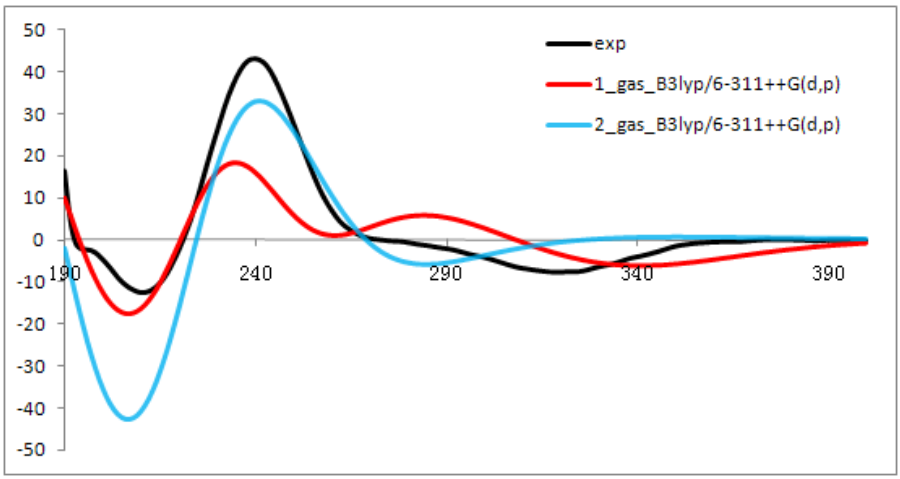

Fig. S8. Calculated ECD spectra of cyclopenicillone (**1**) and the C-1′ epimer (**2**) at B3LYP-SCRF/6-311++G**//B3LYP/6-31G** level with the PCM model in methanol

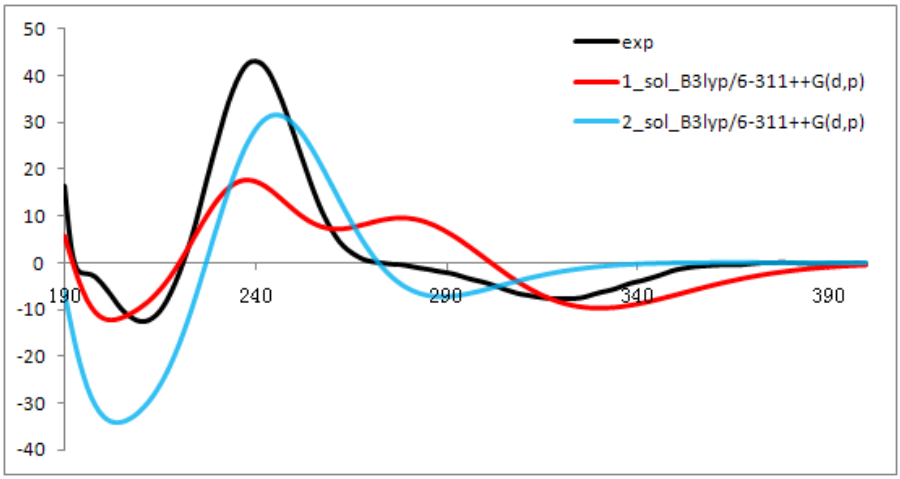

This journal is © The Royal Society of Chemistry 2011

Fig. S9. Key molecular orbitals involved in the important transitions in ECD of conformer **2d** at B3LYP-SCRF/6-31G**//B3LYP/6-31G** level with the PCM model in methanol.

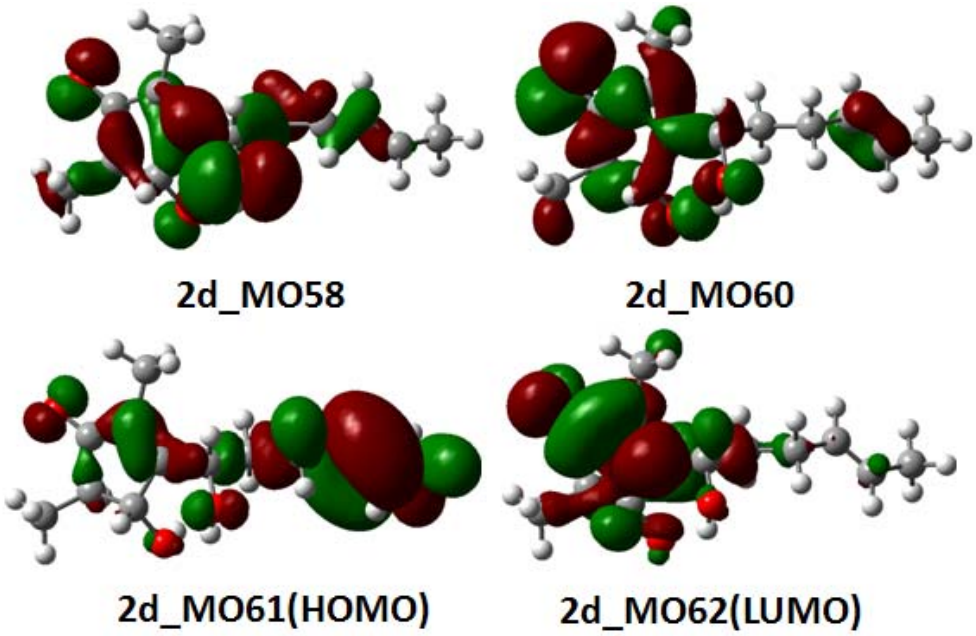

Table S1. Important dihedral angles of optimized cyclopenicillone (**1**) at B3LYP/6-31G** Level in the Gas Phase (Degree)

	4-3-1′-O	4-3-1′-2′	3-1′-2′-3′	1′-2′-3′-4′	2′-3′-4′-5′	3′-4′-5′-6′
1a	9.7	-115.1	-178.3	177.9	118.7	179.9
1b	10.4	-109.9	-177.8	-176.8	-117.2	180.0
1c	55.1	-70.3	-177.1	-179.9	118.1	-179.7
1d	54.9	-70.5	-175.7	175.7	-118.5	-179.9
1e	6.3	-115.1	60.8	173.3	117.8	-179.8
1f	6.3	-115.1	61.3	179.0	-117.3	179.6
1g	-152.4	81.3	61.3	71.6	115.4	179.8
1h	-161.3	69.0	62.5	68.6	-127.3	-177.6
1i	-147.9	84.9	-176.1	179.8	118.4	-179.9
1j	-146.6	86.2	-175.8	179.0	-117.2	-179.9
1k	9.0	-111.5	-178.6	179.5	-0.6	179.9
1l	6.9	-114.6	61.5	176.8	0.9	-179.9

Table S2. Important thermodynamic parameters of cyclopenicillone (**1**) (au)

Species	In Gas Phase					In Methanol
	E	E′=E+ZPE	H	G	Es	Esol
1a	-733.098826	-732.788398	-732.769249	-732.835940	-733.110186	-733.301339
1b	-733.098799	-732.788581	-732.769317	-732.836906	-733.110060	-733.301193
1c	-733.099705	-732.789462	-732.770053	-732.837916	-733.110857	-733.301645
1d	-733.099732	-732.789339	-732.770001	-732.837371	-733.110916	-733.301729
1e	-733.098321	-732.787636	-732.768635	-732.834932	-733.109656	-733.300419
1f	-733.098097	-732.787728	-732.768571	-732.835696	-733.109486	-733.300266
1g	-733.091583	-732.781457	-732.762169	-732.829157	-733.103096	-733.292986
1h	-733.094580	-732.783928	-732.765010	-732.830540	-733.106004	-733.294530
1i	-733.093937	-732.783877	-732.764554	-732.831338	-733.106495	-733.296890
1j	-733.093788	-732.783818	-732.764455	-732.831517	-733.106418	-733.296940
1k	-733.097492	-732.787070	-732.767927	-732.834582	-733.108766	-733.299741
1l	-733.096760	-732.786276	-732.767218	-732.833688	-733.108181	-733.298722

*E, E′, H, G: total energy, total energy with zero point energy (ZPE), enthalpy and Gibbs free energy in the gas phase at B3LYP/6-31G** level;* E_s*: single point energy in methanol at B3LYP/6-31G**//B3LYP /6-31G** level with PCM model;* E_{sol}*: single point energy in methanol solution at B3LYP-SCRF/6-311++G**//B3LYP/6-31G** level with PCM model.*

Table S3. Conformational analysis of cyclopenicillone (**1**)

Species	In Gas Phase								In Methanol	
	ΔE^a	$P_E\%^b$	$\Delta E'^c$	$P_{E'}\%^d$	ΔG^e	$P_G\%^f$	ΔE_s^g	$P_{Es}\%^h$	ΔE_{sol}^i	$P_{Esol}\%^j$
1a	0.57	11.7	0.67	10.7	1.24	5.6	0.46	13.3	0.24	17.5
1b	0.59	11.4	0.55	13.0	0.63	15.5	0.54	11.6	0.34	15.0
1c	0.02	29.7	0.00	33.1	0.00	45.3	0.04	27.1	0.05	24.2
1d	0.00	30.6	0.08	29.1	0.34	25.4	0.00	28.8	0.00	26.4
1e	0.89	6.9	1.15	4.8	1.87	1.9	0.79	7.6	0.82	6.6
1f	1.03	5.4	1.09	5.3	1.39	4.3	0.90	6.3	0.92	5.6
1g	5.11	0.0	5.02	0.0	5.50	0.0	4.91	0.0	5.49	0.0
1h	3.23	0.1	3.47	0.1	4.63	0.0	3.08	0.2	4.52	0.0
1i	3.64	0.1	3.50	0.1	4.13	0.0	2.77	0.3	3.04	0.2
1j	3.73	0.1	3.54	0.1	4.02	0.1	2.82	0.2	3.01	0.2
1k	1.41	2.8	1.50	2.6	2.09	1.3	1.35	3.0	1.25	3.2
1l	1.87	1.3	2.00	1.1	2.65	0.5	1.72	1.6	1.89	1.1

*[a,c,e] Relative energy, relative energy with ZPE, and relative Gibbs free energy at B3LYP/6-31G** level in the gas phase, respectively (kcal/mol). [b,d,f] Conformational distribution calculated by using the respective parameters above at B3LYP/6-31G** level in the gas phase. [g,h] Relative energy (kcal/mol) and conformational distribution in the gas phase at B3LYP/6-311++G** //B3LYP/6-31G** level. [I,j] Relative energy (kcal/mol) and conformational distribution in methanol solution at B3LYP-SCRF /6-31G**//B3LYP/6-31G** level with PCM model, respectively.*

Table S4. Important dihedral angles of optimized cyclopenicillone (**1**) and the C-1′ epimer (**2**) at B3LYP/6-31G** Level in the Gas Phase (Degree)

	H-C1′-C2′-H	O-C4-C1'-O		H-C1′-C2′-H	O-C4-C1'-O
1a	178.8	-45.4	**2a**	-64.6	110.3
1b	178.8	-45.3	**2b**	178.3	78.3
1c	-178.8	7.3	**2c**	59.2	127.3
1d	-178.3	-171.9	**2d**	-65.4	-60.5
1e	54.7	-45.9	**2e**	-179.9	-65.3
1f	55.2	-46.6	**2f**	59.2	-52.9
1g	54.3	175.6			
1h	55.6	162.7			
1i	179.6	-76.8			
1j	-179.3	-174.5			
1k	177.9	-46.0			
1l	55.3	-45.8			

Table S5. Key Transitions, Oscillator Strengths, and Rotatory Strengths in the ECD Spectra of Conformer **1a**, **1b**, **1c** and **1d** in the MeOH with PCM at B3LYP-SCRF/6-31G**//B3LYP/6-31G** Level

Species	Exited State	ΔE^a(eV)	λ^b(nm)	f^c	$R_{vel}{}^d$	$R_{len}{}^e$
1a	60 -> 62	3.7788	328.10	0.0016	-16.6498	-20.4044
	61 -> 62	4.5834	270.51	0.1076	28.9488	30.6011
	59 -> 62	4.9276	251.61	0.0881	-33.1241	-35.4911
	58 -> 62	5.2342	236.87	0.0662	71.7008	76.7945
	57 -> 62	5.8738	211.08	0.1792	-17.8290	-20.8281
	60 -> 64	6.4956	190.87	0.0023	-12.3361	-9.0285
1b	60 -> 62	3.7783	328.14	0.0015	-16.7779	-20.6250
	61 -> 62	4.5548	272.21	0.0631	9.3107	10.2756
	59 -> 62	4.9173	252.14	0.1210	-37.6818	-39.9232
	58 -> 62	5.2558	235.90	0.0576	64.4280	68.9874
	57 -> 62	5.8733	211.10	0.1740	-35.4734	-39.8482
	60 -> 64	6.5104	190.44	0.0013	-12.2129	-8.6164
1c	60 -> 62	3.7694	328.92	0.0017	-14.7998	-17.3931
	61 -> 62	4.6163	268.58	0.0642	28.5325	29.0632
	58 -> 62	5.0889	243.64	0.0010	-5.5247	-7.2637
	57 -> 62	5.3440	232.01	0.0042	-3.8080	-2.8908
	59 -> 62	5.5319	224.13	0.3972	14.7355	16.0178
	60 -> 64	6.5202	190.16	0.0016	-0.2070	2.5882
1d	60 -> 62	3.7683	329.02	0.0018	-15.0751	-17.6344
	61 -> 62	4.5484	272.59	0.0426	18.7172	18.8801
	58 -> 62	5.1613	240.22	0.0043	-13.2865	-14.7078
	57 -> 62	5.3525	231.64	0.0038	-2.7016	-1.8443
	59 -> 62	5.5278	224.29	0.3946	-0.1061	-0.3035
	60 -> 64	6.5249	190.02	0.0013	-5.5655	-2.9598

[a] Excitation energy. [b] Wavelength. [c] Oscillator strength. [d] Rotatory strength in velocity form (10^{-40}cgs.) [e] Rotatory strength in length form (10^{-40}cgs.).

Table S6. Key Transitions, Oscillator Strengths, and Rotatory Strengths in the ECD Spectra of Conformer **2a**, **2b**, **2d** and **2f** in the MeOH with COSMO at B3LYP-SCRF/6-31G**//B3LYP/6-31G** Level

Species	Exited State	ΔE^a(eV)	λ^b(nm)	f^c	$R_{vel}{}^d$	$R_{len}{}^e$
2a	60 -> 62	3.8406	322.82	0.0020	-14.9877	-19.3774
	61 -> 62	4.7094	263.27	0.1028	24.8963	25.0954
	58 -> 62	5.0836	243.89	0.0065	21.1117	22.6020
	59 -> 62	5.4949	225.63	0.3441	-38.3064	-45.2292
	57 -> 62	5.6095	221.03	0.0049	3.9802	5.0321
	60 -> 64	6.5627	188.92	0.0025	5.2264	8.9617
2b	60 -> 62	3.7955	326.66	0.0008	-1.0421	-5.6801
	61 -> 62	4.5836	270.49	0.0201	11.2979	11.8535
	58 -> 62	5.0215	246.91	0.0068	23.1342	25.5012
	57 -> 62	5.3697	230.90	0.2494	18.9587	17.5257
	59 -> 62	5.6516	219.38	0.1167	-27.7937	-29.0459
	60 -> 64	6.4608	191.90	0.0041	10.5127	13.9224
2d	60 -> 62	3.8524	321.84	0.0009	7.1511	2.8654
	61 -> 62	4.6649	265.78	0.1064	-32.2039	-33.1934
	59 -> 62	5.2239	237.34	0.1569	97.7114	104.1355
	58 -> 62	5.2539	235.99	0.0088	-18.5084	-17.4669
	57 -> 62	5.7644	215.09	0.1776	-46.9612	-48.9462
	60 -> 64	6.5706	188.70	0.0138	-40.7052	-36.3083
2f	60 -> 62	3.8368	323.14	0.0006	0.1862	-3.9237
	61 -> 62	4.5898	270.13	0.1071	0.4328	0.6650
	59 -> 62	5.1340	241.50	0.0737	-16.3498	-16.6545
	58 -> 62	5.2681	235.35	0.0533	85.1416	91.7845
	57 -> 62	5.7826	214.41	0.1761	-41.6237	-42.4444
	60 -> 64	6.5260	189.98	0.0099	-35.8768	-31.9015

[a] Excitation energy. [b] Wavelength. [c] Oscillator strength. [d] Rotatory strength in velocity form (10^{-40}cgs.) [e] Rotatory strength in length form (10^{-40}cgs.).

Table S7. The ihibitory activity of cyclopenicillone (**1**) against LPS-induced NO production in RAW264.7 macrophages

Compound	Concentration /μM	Mean±SD	Inhibitory rate (%)	IC_{50}/μM
DMSO	0.5%	0.63±0.27		
LPS	1μg/ml	10.49±0.73	0	
	100	2.40±0.25	77	
cyclopenicillone	50	5.93±0.12	44	
(**1**)	25	8.56±0.23	18	55.49
	10	10.25±0.17	2	
	5	11.77±0.29	-12	
Positive control[a]	100	1.02±0.19	90	20

[a]AG: aminoguanidine (≥98.0%, Sigma)

This journal is © The Royal Society of Chemistry 2011

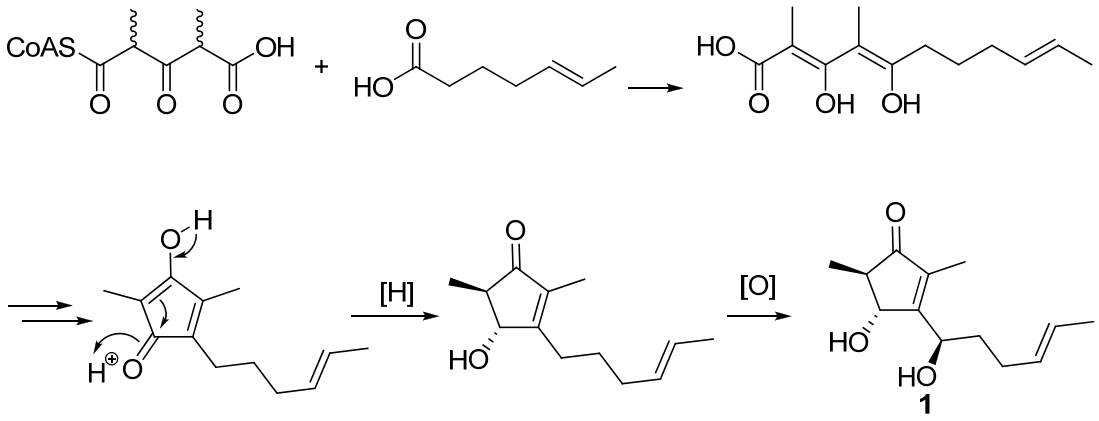

Scheme 1. Postulated Biogenetic Formation of cyclopenicillone (1)

Fig. S10. The Positive mode HRESI Spectrum of Cyclopenicillone (1)

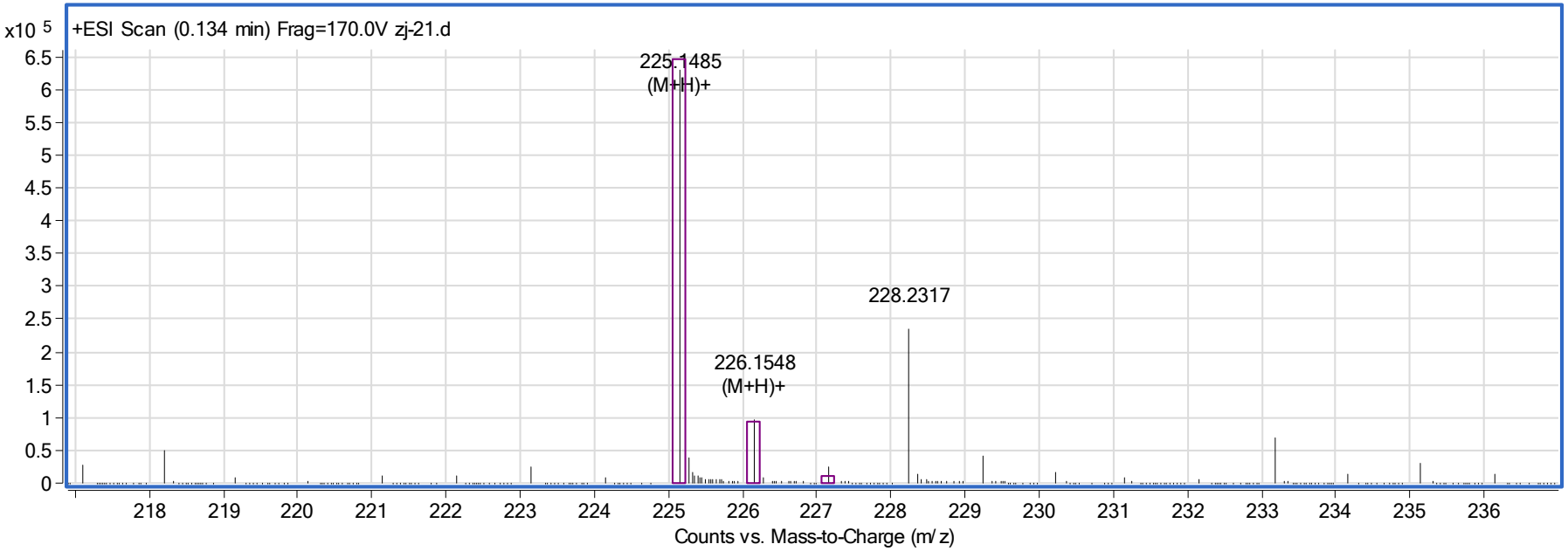

m/z	Ion	Formula	Abundance
225.1485	(M+H)+	C13 H21 O3	628367.6

Best	Formula (M)	Ion Formula	Calc m/z	Score	Cross Score	Mass	Calc Mass	Diff (ppm)	Abs Diff (ppm)	Abund Match	Spacing Match	Mass Match	m/z	DBE
☑	C13 H20 O3	C13 H21 O3	225.1485	90.3		224.1413	224.1412	-0.09	0.09	92.82	67.9	100	225.1485	4

Fig. S11. The IR Spectrum of Cyclopenicillone (1)

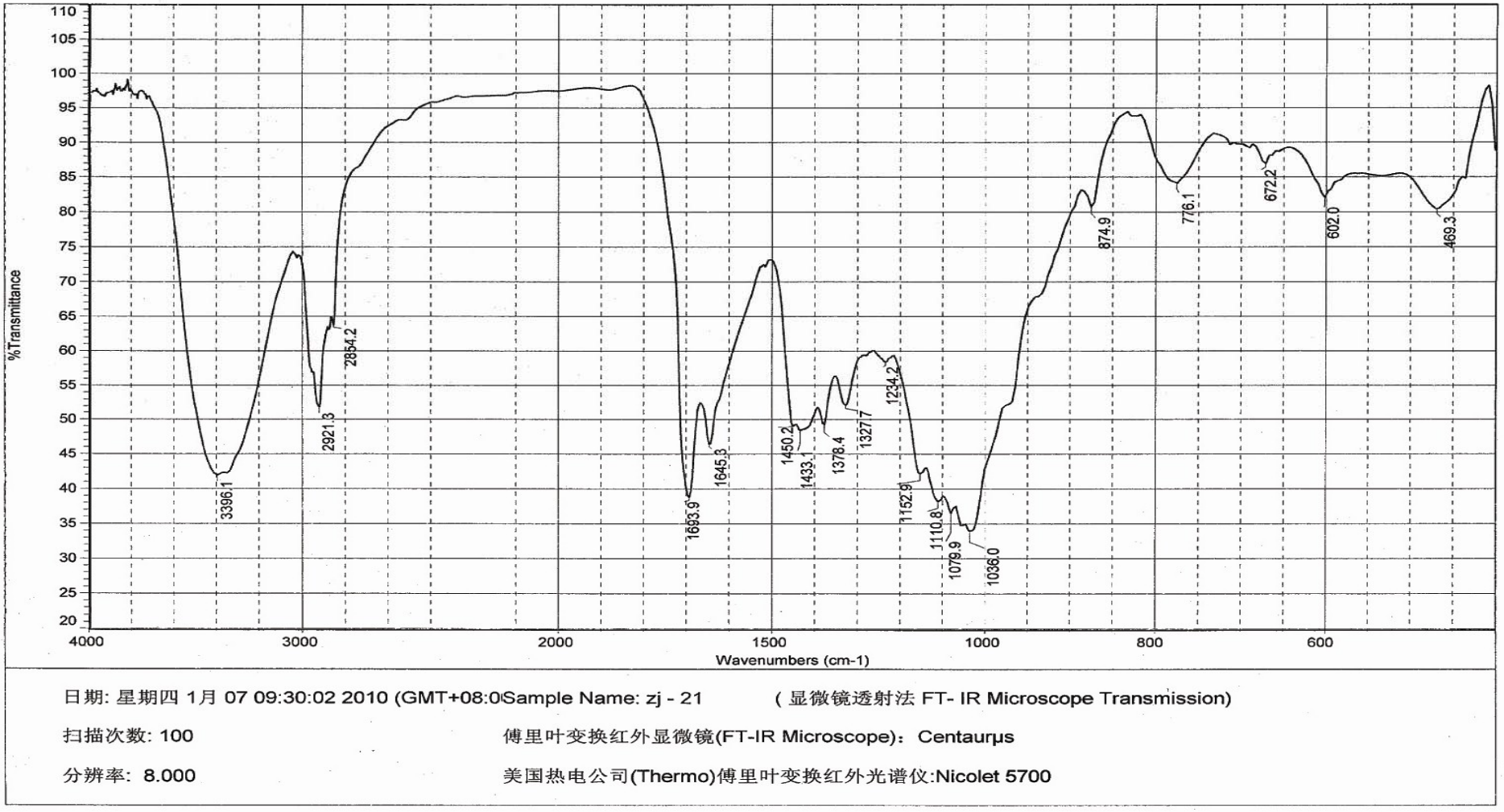

Fig. S12. The IR Spectrum of Cyclopenicillone (1) in a diluted concentration

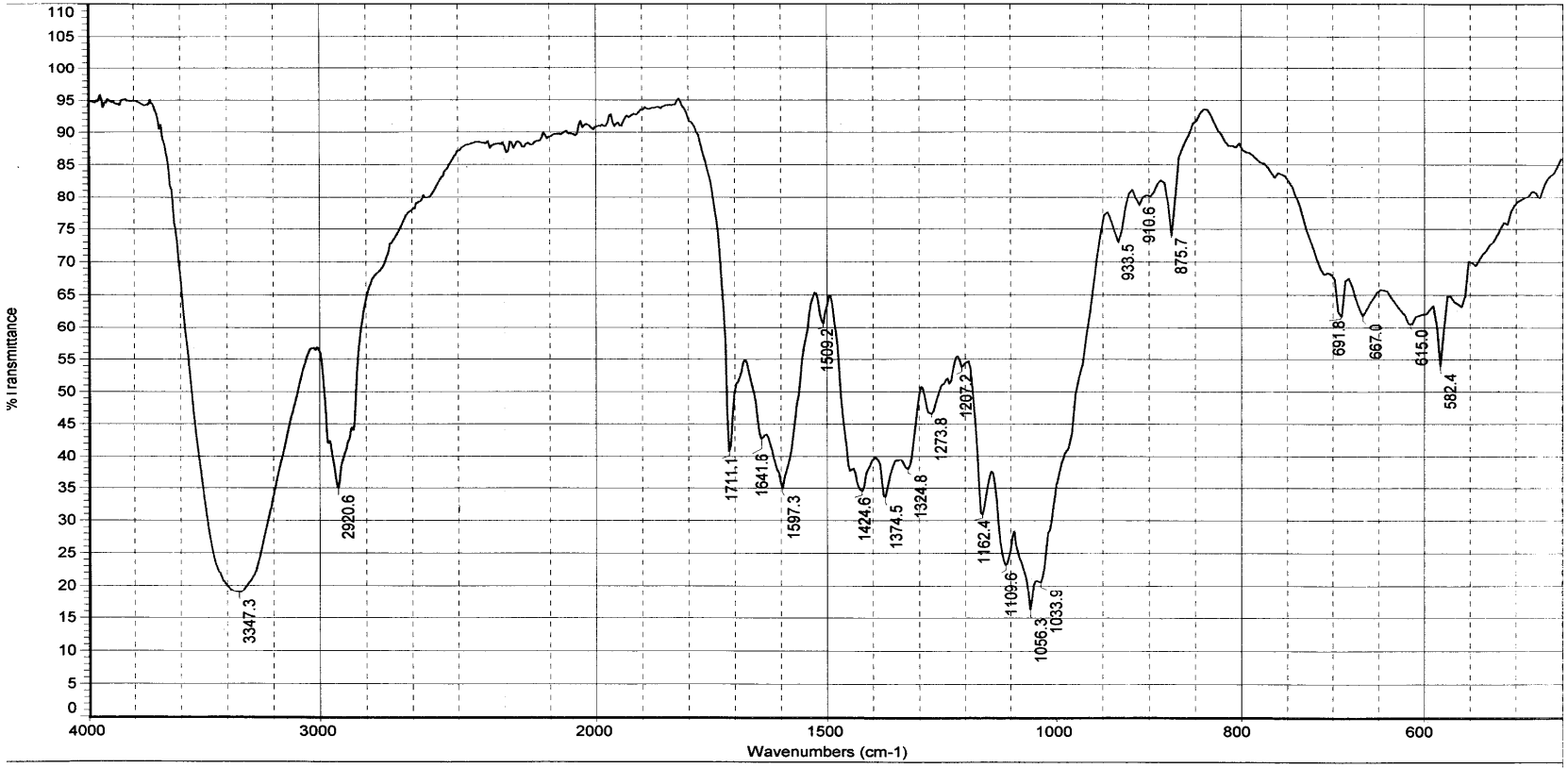

日期: 星期二 5月 24 11:43:21 2011 (GMT+08:0 Sample Name : ZJ - 21 （显微镜透射法 FT- IR Microscope Transmission)

扫描次数: 100 傅里叶变换红外显微镜(FT-IR Microscope)：Centaurμs

分辨率: 8.000 美国热电公司(Thermo)傅里叶变换红外光谱仪:Nicolet 5700

Fig. S13. The ^{1}H NMR Spectrum of Cyclopenicillone (1) in MeOH-d_4

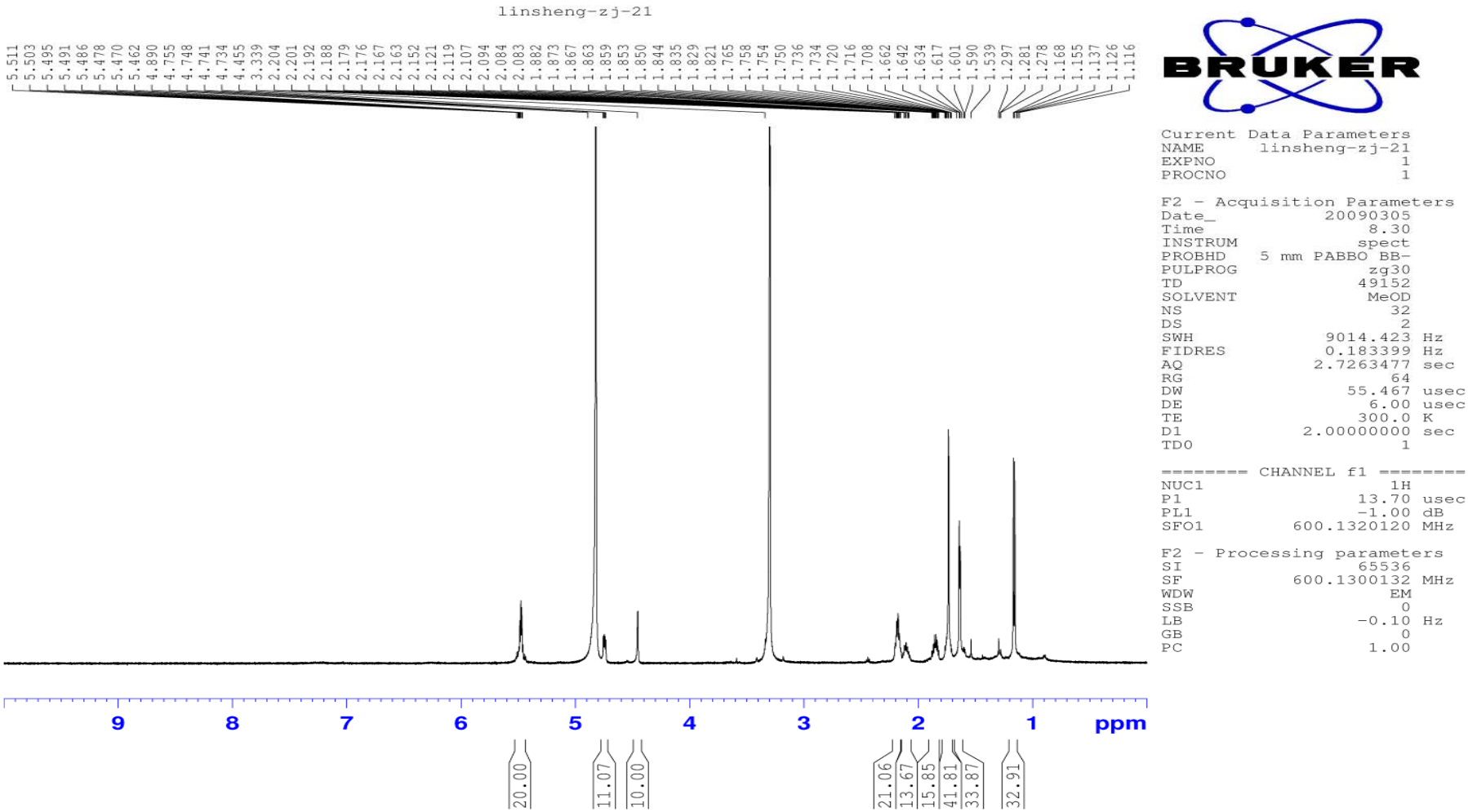

Fig. S14. The ^{13}C and DEPT NMR Spectra of Cyclopenicillone (1) in MeOH-d_4

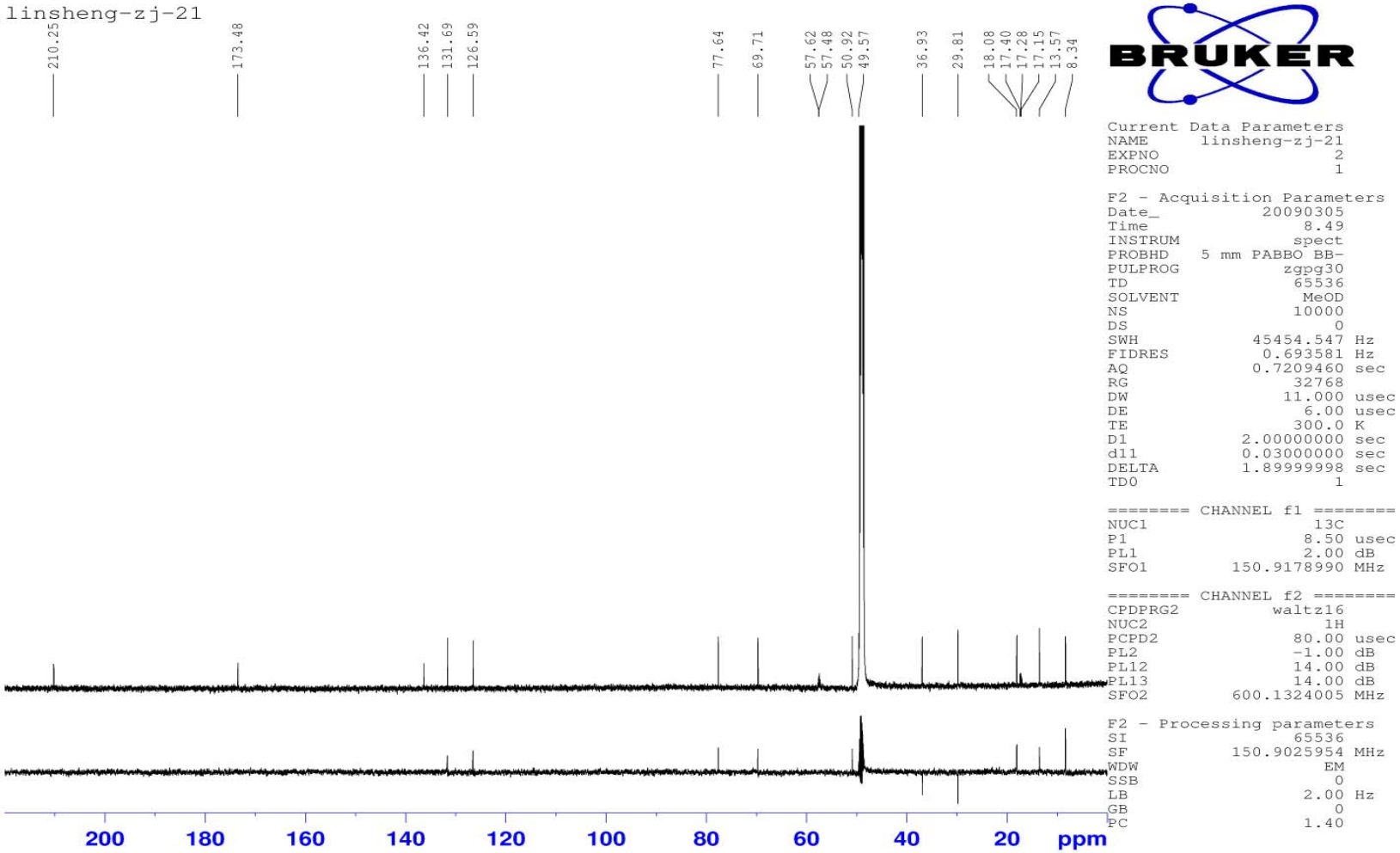

Fig. S15. The ^{1}H-^{1}H COSY Spectrum of Cyclopenicillone (1) in MeOH-d_4

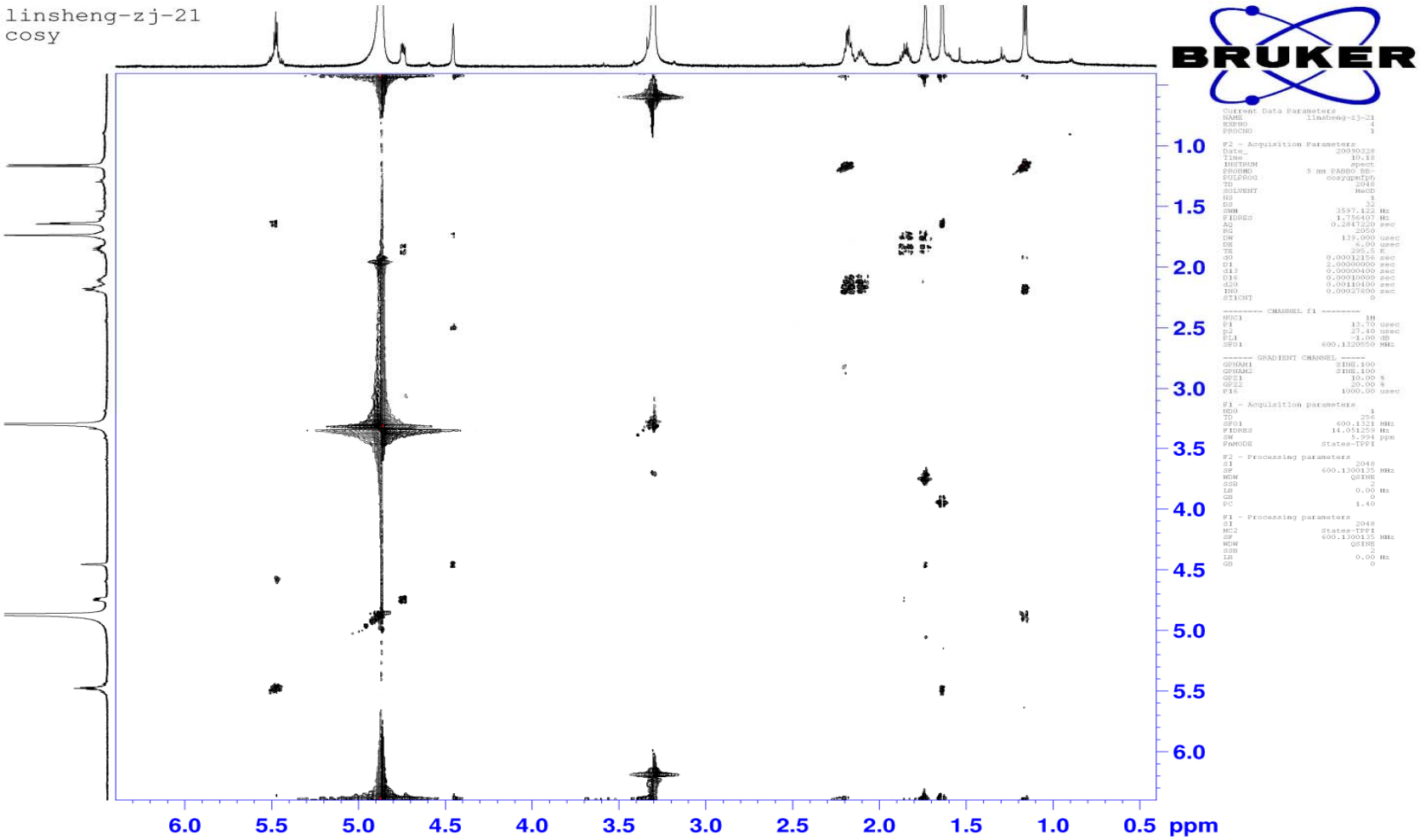

Fig. S16. The HSQC Spectrum of Cyclopenicillone (1) in MeOH-d_4

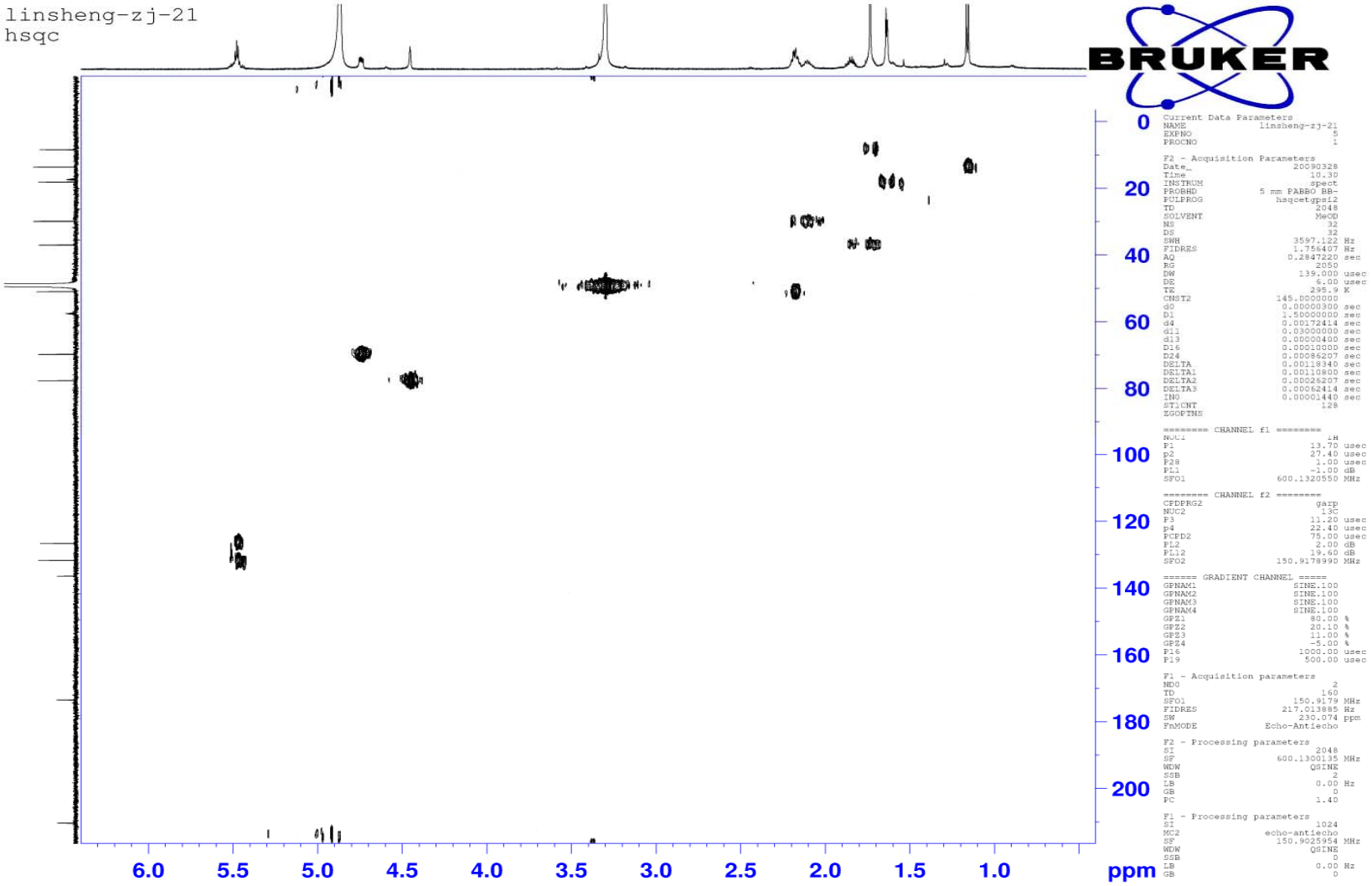

Fig. S17. The HMBC Spectrum of Cyclopenicillone (1) in MeOH-d_4

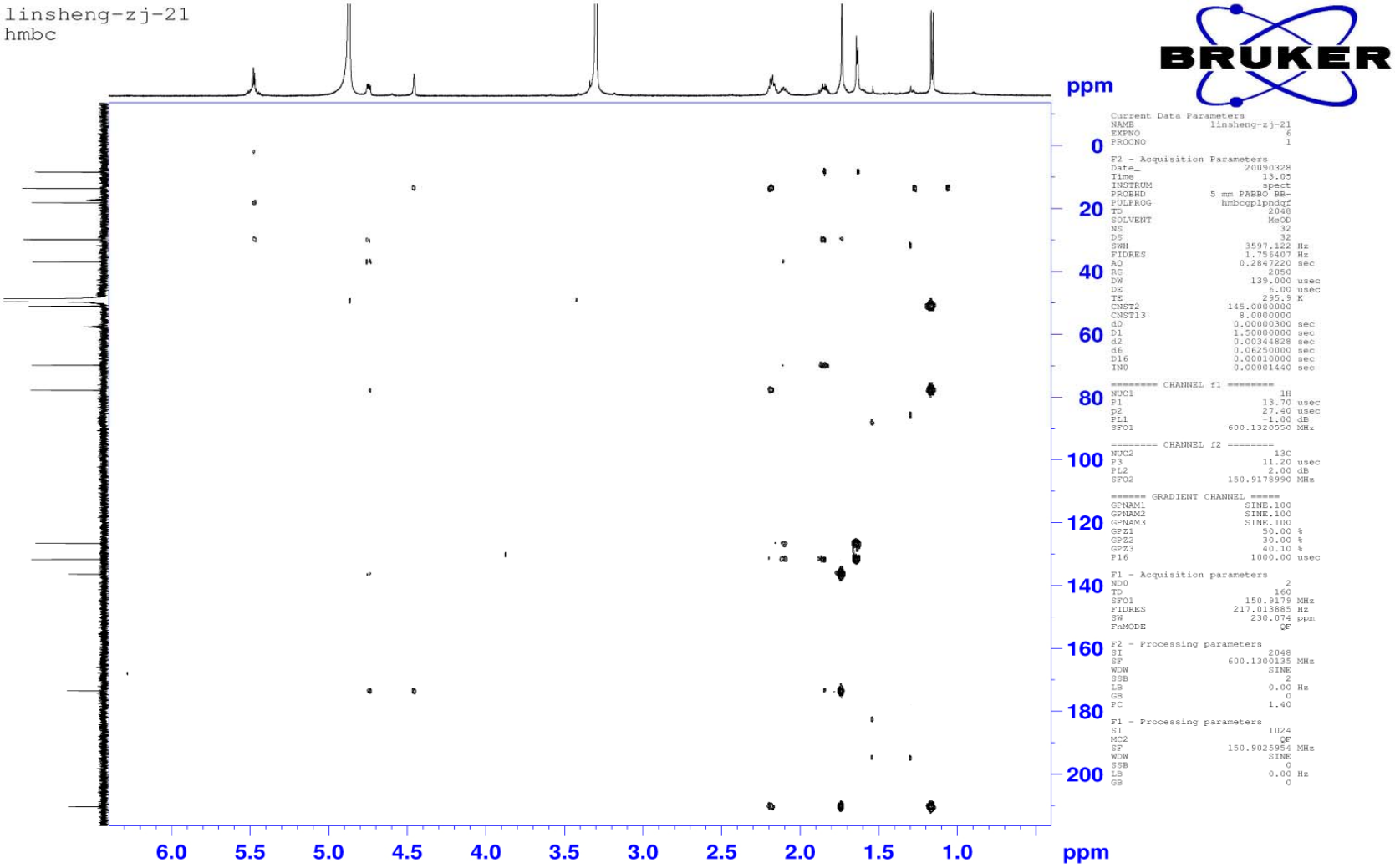
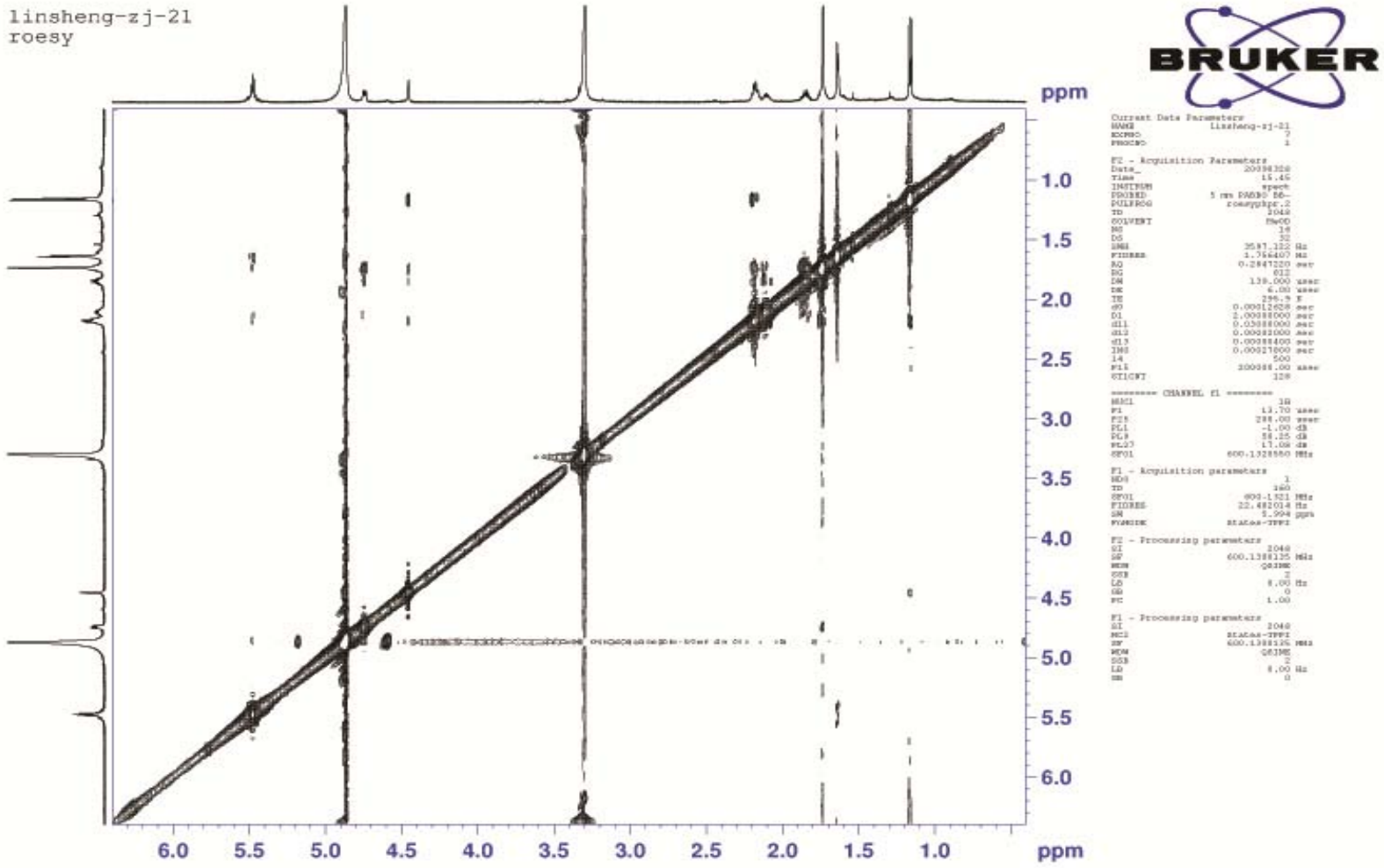
Fig. S18. The ROESY Spectrum of Cyclopenicillone (1) in MeOH-d_4